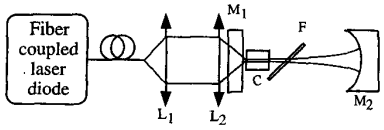

CThJ5 Fig. 1. Experimental setup. L_1, L_2: collimating and focusing 60-mm doublets. M_1: input mirror. M_2: output mirror. C: Yb:GdCOB crystal. F: Lyot filter.

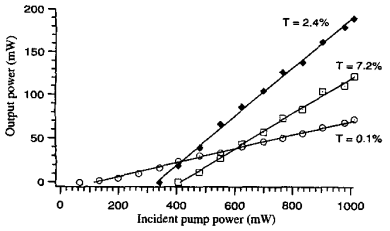

CThJ5 Fig. 2. Performances of the diode-pumped Yb:GdCOB laser with different output couplers.

in our experiments. The sample was anti-reflection coated around 1030 nm on both sides and sandwiched between two copper blocks. The crystal temperature could be stabilized at 6°C for power measurements or changed from 6°C to 55°C to study its influence on the laser performances. As pump source (cf. Fig. 1), we used a 1.2 W fiber-coupled laser diode (OPC H01A001-901-FC) emitting at 901 nm (M^2 = 18). The pump optics gave a 65-μm waist inside the crystal. The cavity was formed by a plane dichroïc mirror (HR around 1030 nm, HT at 900 nm) and a concave output coupler with a 100-mm radius of curvature and various transmissions (T = 0.1%, 2.4% and 7.2%). The cavity waist was around 55-μm and 56% of the pump ligth was absorbed in the crystal.

As shown in Fig. 2, even with a 7.2% output coupler, an high laser effect has been obtained. It proves that important small signal gain can be achieved under diode-pumping. With a 2.4% output coupler, 191 mW at 1050 nm for 600 mW of absorbed pump power have been demonstrated (slope efficiency of 47.5%) at 6°C with a laser threshold of 116 mW. Due to the importance of the crystal temperature in a quasi-three level laser, its influence has been studied. Only 30% in output power were lost as the crystal temperature increased by 50°C. Compared with YAG, glass or SFAP, those results are much better.[2,4,8]

By inserting a Lyot filter in the cavity and with a 1.7% output coupler (because of important losses on the filter), we achieved tunability of the Yb:GdCOB laser from 1035 nm to 1088 nm with a maximum output power of 120 mW at 1082 nm at 6°C (cf. Fig. 3). Using a low transmission mirror (T = 0.03%), a 102-nm tunability was obtained (from 1013 nm to 1115 nm) which is, to our knowledge, the largest range ever obtained with Yb doped materials.

In conclusion, we believe this to be the first demonstration of an efficient tunable cw diode-pumped Yb:GdCOB laser. These high

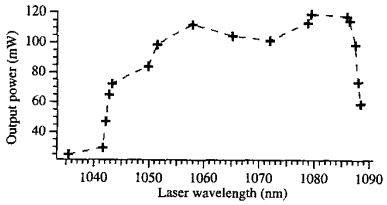

CThJ5 Fig. 3. Output power versus laser wavelength.

performances may found applications for developing microchip lasers or high average power pulsed lasers. Works are underway on the Q-switch regime. We also plan to work on the development of a compact femtosecond source based on diode-pumped Yb:GdCOB crystal.

Chimie Appliquée de l'État solide, ENSCP, 11 rue Pierre et Marie Curie, 75231 Paris Cedex 05 France and Crismatec, BP 521, 77794 Nemours Cedex - France

**Chimie Appliquée de l'État solide, ENSCP*

1. T.Y. Fan, S. Klunk, G. Henein, Opt. Lett. **18,** 423 (1993).
2. M.R. Dickinson, L.A.W. Gloster, N.W. Hopps, T.A. King, Opt. Com. **132,** 275 (1996).
3. L.A.W. Gloster, P. Cormont, A.M. Cox, T.A. King, B.H.T. Chai, Opt. Com. **146,** 177 (1998).
4. C. Hönninger, F. Morier-Genoud, M. Moser, U. Keller, Opt. Lett. **23,** 126 (1998).
5. G. Aka, A. Kahn-Harari, D. Vivien, J-M. Benitez, F. Salin, J. Godard, Eur. J. Sol. Stat. Inorg. Chem. **33,** 727 (1996).
6. G. Aka, L. Bloch, J. Godard, A. Kahn-Harari, D. Vivien, F. Salin and Crismatec company, Cristaux non linéaires et leur applications French Patent n° FR 95/01963 (1995), European Patent extension n° 96904152.4-2205 (1996), International patent extension pending.
7. F. Mougel, K. Dardenne, G. Aka, A. Kahn-Harari, D. Vivien, J. Opt. Soc. Am B **16,** 1 (1999) (in press).
8. T. Kasamatsu, H. Sekita, A. Kuwano, in Advanced Solid State Laser, OSA TOPS **19,** 125 (1998).

CThJ6 **11:45 am**

Diode-pumped Yb^{3+}:$Sr_5(VO_4)_3F$ laser

A.N.P. Bustamante, D.A. Hammons, R.E. Peale, M. Richardson, B.H.T. Chai, A. Chin,* J. Cary,* *Center for Research and Education in Optics and Lasers, University of Central Florida, 4000 Central Florida Blvd., Orlando, Florida 32816-2700 USA; E-mail: andrea@mail.creol.ucf.edu*

Recent publications show high slope efficiencies, high emission cross section, and low laser threshold for Yb^{3+} in appatite host structures.[1–6] We have developed a Czochralski technique for producing SVAP crystalline boules with up to 6% Yb (by weight in the starting melt). Contrary to common practice in growing oxyfluoride crystals, high oxidation in the growth atmosphere produces better

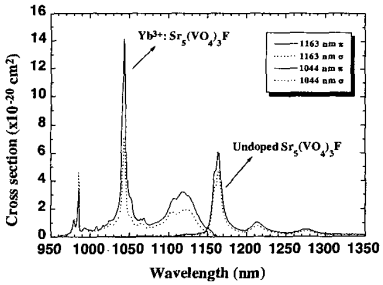

CThJ6 Fig. 1. Polarized emission spectra for the laser lines at 1044 nm and 1120 nm in Yb^{3+}: SVAP.

quality SVAP single crystals. Large crystalline boules were grown without the tendency toward grain boundaries, cracks, or spiraling, suggesting that our method can make this host market-ready.

Diode-pumped operation of Yb^{3+}:SVAP was achieved for the first time by generating emission at 906 nm from a new high brightness, InGaAs/AlGaAs laser diode which overlapped well with the broad absorption at 905 nm. Polarized photoluminescence of Yb^{3+}:SVAP shows a narrow line at 1044 nm, and a broad emission at 1120 nm (Fig. 1). The measured lifetime of the Yb^{3+}:SVAP is 544 μs, which occurred in a single exponential decay. A previously unobserved emission band at 1163 nm is also evident in Fig. 1. Its emission cross section is calculated assuming its origin is from undoped SVAP with a different lifetime 320 μs. Additional experiments are being performed to understand the origin of this emission.

Initial laser action in Yb^{3+}:SVAP was investigated with a 6% doped uncoated handpolished 5 × 5 × 9 mm laser crystal mounted on a thermoelectric cooler. Continuous-wave laser operation was achieved using an end-pumped hemispherical linear cavity consisting of a flat high reflector and a 10-cm radius of curvature output coupler. A tunable Ti:Sapphire capable of 1.5 W of power at 905 nm was focused into the crystal through the rear mirror, which was 95% transparent at 905 nm. The pump beam was focused with an 8.8-cm focal length lens to a ~70 μm (FWHM) spot size. We achieved a slope efficiency of 57% with a 20% output coupling at 1044 nm.

Diode pumped experiments was performed to demonstrate and characterize laser operation at both 1044 nm and 1120 nm. The diode was capable of more than 1.6 W at 906 nm. Using a similar hemispherical laser resonator, laser operation was achieved at 1043.6 nm and 1117 nm. The Yb^{3+}:SVAP laser rod (5 × 5 × 9 mm) was placed close to the high reflector and a nominal output coupling of 1% was used in both experiments. Having collimated the diode pump beam, a 60 mm focal length lens was used to focus the pump beam to ~100 μm (FWHM). The diode-pumped laser output power at 1044 nm as a function of absorbed pump power is shown in Fig. 2. A slopeefficiency of 12% was achieved with 34 mw of output power. Operation of the 1120 nm band corresponded with a broad laser emission cen-

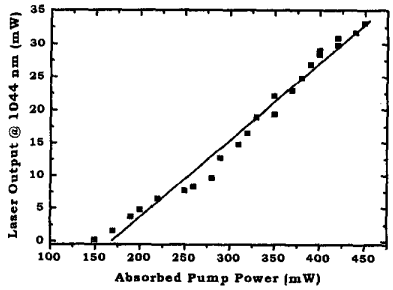

CThJ6 Fig. 2. Laser output power at 1044 nm as a function of absorbed 905 nm pump power in 6% Yb^{3+}:SVAP.

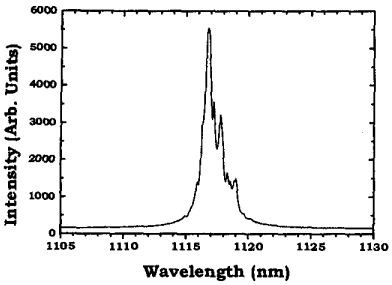

CThJ6 Fig. 3. Laser emission of diode-pumped Yb^{3+}:SVAP at 1117 nm.

tered at 1117 nm (Fig. 3). More than 5 mW of output power was achieved.

Diode-pumped laser operation of Yb^{3+}:SVAP has been successfully demonstrated for the first time at 1044 nm and 1117 nm. We expect tunable laser action and ultra-short operation in the femtosecond regime in the broadband emission at 1120 nm.

Polaroid Corporation, 1 Upland Road, Norwood, Massachusetts 01062 USA

1. S.A. Payne, L.D. DeLoach, L.K. Smith, W.F. Krupke, B.H.T. Chai and G. Loutts, *Advanced Solid State Lasers, OSA Proceedings Series*, vol. **20,** Tso Yee Fan and Bruce H.T. Chai (eds.), Optical Society of America, 1994.
2. L.D. DeLoach, S.A. Payne, W.L. Kway, J.B. Tassano, S.N. Dixit and W.F. Krupke, J. Luminescence **62,** 85, 1994.
3. S.A. Payne, L.D. DeLoach, L.K. Smith, W.L. Kway, J.B. Tassano, W.F. Krupke, B.H.T. Chai and G. Loutts, J. Appl. Phys. **76** (1), 497, 1994.
4. P.E. Mackie and R.A. Young, J. Appl Cryst. **6,** 26, 1973.
5. L.D. DeLoach, S.A. Payne, L.L. Chase, L.K. Smith, W.L. Kway and W.F. Krupke, IEEE J. Quantum Electronics **29,** No. 4, 1179, 1993.
6. C.D. Marshall, L.K. Smith, R.J. Beach, M.A. Emanuel, K.I. Schaffers, J. Skidmore, S.A. Payne and B.H.T. Chai, IEEE J. Quantum Electronics, Vol. **32,** No. 4, 650 (1996).

Thursday, May 27

JThB

10:30 am–NOON
Rooms 327/329

Single Cycle Propagation

Xi-Cheng Zhang, *Rensselaer Polytechnic Institute, USA, Presider*

JThB1 **10:30 am**

Propagation effects at the focus of single-cycle terahertz pulses

S. Feng, S. Hunsche,* A. Leitenstorfer,* H.G. Winful, E.P. Ippen,** M.C. Nuss,**
EECS Department, The University of Michigan, 1301 Beal Avenue, Ann Arbor, Michigan 48109-2122 USA; E-mail: sfeng@umich.edu

We investigate experimentally and numerically the temporal profiles of single-cycle pulses passing through a focus. Both experimental and numerical results show significant pulse shaping, time reversal, and superluminal propagation as a pulse evolves through the focus.

One of the most striking phenomena associated with the focusing of electromagnetic beams is the Gouy phase shift. This phase shift has been predicted to lead to pulse reshaping, polarity reversal, and time reversal as terahertz pulses evolve through a focus.[1,2] It has also been suggested that this same Gouy shift should result in superluminal pulse propagation along the optical axis within the Rayleigh range of the pulse.[3] In this paper we report experimental results that show the predicted pulse shaping, time reversal, and apparent propagation at a speed greater than the velocity of light in vacuum as a terahertz pulse passes through a focus. The experimental results agree well with simulations based on the time-domain Kirchhoff diffraction integral.

The experimental arrangement is shown in Fig. (1). Terahertz pulses are created in a GaAs emitter biased by a gold stripline. The THz radiation is coupled into space by an aplanatic hyper-hemispherical silicon substrate lens, collimated by an off-axis paraboloid mirror and focused by a second paraboloid with a focal length of 7.5 cm. The THz detector consists of a conventional photoconductive dipole antenna with 50 μm dipole length fabricated on ion-implanted silicon-on-sapphire. Since the dipole size is much smaller than the wavelength of the radiation, it can be assumed to act as a simple point probe of the THz field. The detector is moved through the focal region along the propagation axis z with a stepper

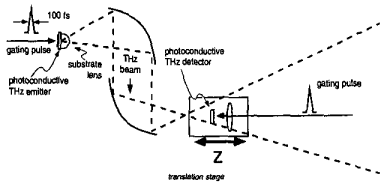

JThB1 Fig. 1. Experimental setup for the terahertz pulse.

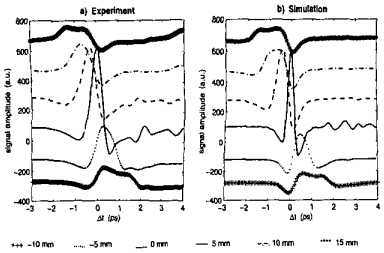

JThB1 Fig. 2. Experimental (a) and theoretical (b) THz temporal waveforms at several positions along axis z. The pulse propagates from the points before the focus ($z < 0$), passing through the focus ($z = 0$), to the points after the focus ($z > 0$). Individual traces are offset for clarity.

motor. A second stepper motor-driven delay line compensates the time delay offset due to the z-motion of the detector, so that the THz field is measured as a function of the local time of the propagating pulse, $\Delta t = t - z/c$.

Figure 2(a) shows the measured THz waveforms (a) and simulations (b) obtained with the model described below for several positions along the optical axis, where $z = 0$ is the focal point. The direction of z corresponds to the propagation direction of the THz pulse, i.e. positive values indicate positions behind the focal plane. Waveforms at similar positive and negative z appear to be very similar if one assumes reverse direction of the time axis, and there is an overall change in pulse shape from an anti-symmetric to a symmetric pulse and back, as predicted by theory. However, the experiment does not show a complete sign reversal of the pulse, and the distortions are not completely symmetric with respect to $z = 0$, so that the pulse at $+15$ mm most closely resembles the one at -10 mm. Very remarkably, the pulses seem to propagate forward in local time while going from negative to positive z, i.e. seem to propagate faster than the speed of light. The measured velocity is greater than the speed of light in vacuum by about 2%.

Since the wave in the collimated region is approximately a plane wave, in the simulation the pulse focusing is modeled by a plane wave incident upon a spherical mirror, and the time-domain Kirchhoff diffraction integral is used to calculate the field on the detector[4]:

$$U(P_0, t) = \int\int_{\Sigma} \frac{\cos(\mathbf{n}, \mathbf{r}_{10})}{2\pi c r_{10}} \frac{d}{dt} U\left(P_1, t - \frac{r_{10}}{c}\right) ds, \quad (1)$$

which gives the field component U at the position of the detector P_0 as a function of t for a given incoming wave on the diffracting screen. The temporal functions on the spherical mirror are obtained by inverse Fourier transforms of the spectra on the mirror which are obtained by fitting the spectrum at the focus ($z = 0$) and multiplied by a Gaussian beam transverse profile.

The observed pulse broadening and the time reversal can be understood geometrically by using the time domain Kirchhoff diffracting integral. All secondary pulses coming from the diffracting screen add up exactly in phase only when the detector is at the focus. When the